



Research article

Analysis of the effect of thermal treatment and catalyst introduction on electrode performance in vanadium redox flow battery

Guanxia Dai ^{a,b,*}, Yanhong Huang ^a, Feihong Chu ^a, Chencong Jin ^a, Hui Liu ^{b,c}^a Department of Electrical Engineering, Hebei Vocational University of Technology and Engineering, Xingtai, 054000, China^b Xingtai Key Laboratory of New Energy Optoelectronic Devices and Energy Storage Technology, Xingtai, 054000, China^c Hebei Yosun New Energy Technology Co., Ltd., Xingtai, 054000, China

ARTICLE INFO

INDEX TERMSP:

Vanadium redox flow battery
Electrode
Carbon felt
Thermal-treat
Noble metal catalyst

ABSTRACT

All-vanadium redox flow batteries (VRFB) have the advantages of high safety and long life, and have broad application prospects in the field of large-scale power energy storage. Low energy density is the main factor restricting its development. In this study, the carbon felt used as the electrode was pretreated in various ways to improve the performance of the vanadium redox flow battery. The pretreatment conditions of carbon felt were compared to the performance of carbon felt after treatment at different temperatures and different times. The properties of the pretreated carbon felt were investigated and their effect on cell performance was tested. Next, by introducing a noble metal catalyst into the carbon felt, the characteristics of the carbon felt were studied and the effect on the performance of the vanadium redox flow battery was investigated. It was found that Carbon felt thermal-treated at 500 °C for 2 h showed the best characteristics and had the longest charge/discharge time and the lowest resistance. The results also show that Carbon felt with catalyst introduced without PTFE (Polytetrafluoroethylene) binder showed larger BET (Brunauer-Emmett-Teller) surface area and electrical conductivity compared to PTFE mixed, and cell performance was also excellent.

1. Introduction

To realize a low-carbon society, fossil fuels are gradually being replaced by clean energy sources, however, the use of new energy sources such as wind and solar power is constrained by environmental factors, making it impossible to steadily and continuously output energy [1]. Due to the capricious nature of renewable power, advanced large-scale energy storage devices are required to make the best use of these renewable energy resources [2]. Rechargeable batteries offer an efficient way to store energy. Available battery technologies include lithium ion, nickel-metal hydride (Ni-MH), lead acid, redox flow and the sodium-sulfur (Na-S) system [3]. Among them, the Vanadium Redox Flow Battery (VRFB) is considered a promising energy-storage solution, which is suitable for stationary applications due to its modular design, good scalability, flexible operation and moderate maintenance cost [4].

The Vanadium Redox Flow Battery (VRFB) is a system that performs charging and discharging through the redox reaction of the active material contained in the electrolyte [5–7]. Unlike traditional secondary batteries, which store electric energy in the electrode

* Corresponding author.

E-mail address: daiguanxia@xpc.edu.cn (G. Dai).<https://doi.org/10.1016/j.heliyon.2024.e33561>

Received 27 April 2024; Received in revised form 8 June 2024; Accepted 24 June 2024

Available online 25 June 2024

2405-8440/© 2024 Published by Elsevier Ltd.

This is an open access article under the CC BY-NC-ND license

<http://creativecommons.org/licenses/by-nc-nd/4.0/>.

containing the active material, the VRFB uses an electrolyte stored in two separate tanks, allowing for a decoupling of power and energy capacity [8]. This design enhances safety, scalability, and resource utilization, making VRFB a suitable choice for large-scale energy storage applications [9,10].

As shown in Fig. 1, the redox flow battery consists of an electrolyte tank (determining the storage capacity of active materials in different oxidation states), a pump (recycling active materials) and a stack responsible for output [5]. In particular, the structure where the electrolyte tank and the stack are separated allows the power and capacity to be freely designed, the installation location is also less restrictive [11]. In addition, no tail gas such as CO_2 is produced, and the vanadium active material in the electrolyte is semi-permanent and reusable, which can effectively use resources [9,12].

Despite its advantages, the VRFB faces challenges such as relatively high and volatile price of vanadium, the cost of raw materials for electrolytes preparation, low energy density and high cost [13–16]. A significant factor influencing the performance of VRFB is the electrode material. Electrodes in VRFB should provide sites for redox reactions, facilitate electron transport, and have low resistance and high redox reaction efficiency [17]. Carbon materials, such as graphite felt, carbon cloth, and carbon fibers, are commonly used as electrodes in VRFB due to their conductivity and chemical stability [13,18].

Recent research has focused on improving the electrochemical performance of VRFB electrodes through various treatment methods and material modifications [19]. Thermal treatment of carbon felt electrodes have been shown to increase surface area, thereby enhancing electrochemical activity [17,20]. Additionally, introducing catalysts, such as noble metals, can further enhance the reaction kinetics and overall performance of the electrodes [21].

This study aims to investigate the effects of thermal treatment and catalyst introduction on the performance of carbon felt electrodes in VRFB. By optimizing the thermal treatment conditions and exploring different catalyst incorporation methods, we aim to enhance the electrochemical properties and overall efficiency of VRFB electrodes.

2. Electrode characteristics and performance improvement of redox flow battery

2.1. Introduction

In Vanadium Redox Flow Battery (VRFB), the electrode should serve to provide a site where a redox reaction can occur, a path for generated electrons, and should have low resistance and good redox reaction efficiency [22]. During the charging process of the VRFB, in the cathode, the V^{4+} is converted into V^{5+} by oxidation reaction, and in the anode, the V^{3+} is converted into V^{2+} by reduction reaction [23]. The discharging process is the opposite of the charging process. Since the electrolyte does not deteriorate, it can be reused semi-permanently. The battery voltage is basically 1.26V [24].

As key materials of vanadium batteries, Carbon materials are used as electrodes for vanadium redox flow batteries. Carbon materials are important parts on supporting the chemical reaction to attain good performance of the VRFB system [13]. In this study, carbon felt used as an electrode was thermal treated in various ways to improve the performance of the vanadium redox flow battery [25]. In addition, the characteristics of pre-treated carbon felt were studied and the effect on cell performance was investigated. Furthermore, by introducing a noble metal catalyst to carbon felt, the characteristics of carbon felt were studied, and the effect on the performance of vanadium redox flow battery was investigated [26].

2.2. Experimental

- (1) Reagents and materials: Vanadium(V) oxide (V_2O_5 , 99.6 %) and Vanadium(IV) oxide sulfate hydrate ($\text{VOSO}_4 \cdot x\text{H}_2\text{O}$, 99.99 %) were obtained from Sigma-Aldrich. Sulfuric acid (H_2SO_4 , 95 %) was purchased from Duksan, pure chemicals Co. Pt/C (20 wt%) was obtained from the Fuel cell store, Pd/C (20 wt%) was purchased from Premetek Co. Carbon felt which is a PAN series, was purchased from the SGL group.
- (2) Thermogravimetric analysis and morphology observation: To check the thermal treatment conditions of carbon felt, a carbon felt sample was placed in a Pressure Thermogravimetric Analyzer (ThermoElectron, TherMax 500) and the temperature was

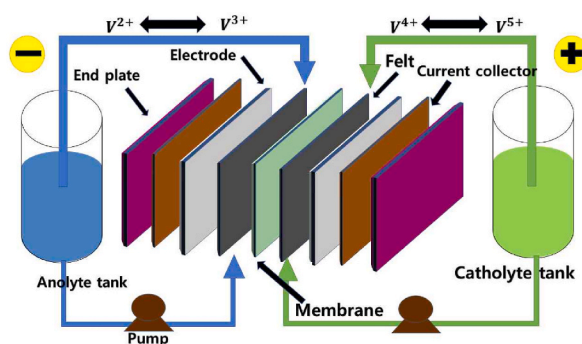


Fig. 1. Experimental apparatus of redox flow battery single cell.

raised from 25 °C to 800 °C in an air atmosphere at a rate of 5 °C/min for thermogravimetric analysis (TGA). FE-SEM(JEOL, JSM-6701F) was used for surface analysis, and EDS(Oxford, INCA M/X)was used for elemental analysis.

- (3) Electrical conductivity: The electrical conductivity was calculated by measuring the electrical resistance by a 4-terminal method using a Conductivity Meter(Keithley, 2182A Nanovoltmeter/6220 Precision Current Source) [3]. For the connection method of resistance measurement, both the 2-terminal method and 4-terminal method are generally used, but to accurately measure low-level resistance, the 4-terminal method must be adopted. As shown in Fig. 2, 4 cables are used to connect the resistance (R_x) and the measuring instrument. The measurement cable also has a resistance value (R_L), which can cause measurement errors. However, Since the internal resistance of the voltmeter is very high, the resistance value R_L of the cable can be ignored.
- (4) Pore distribution and surface area: A MicroPore Physisorption Analyzer (Micrometrics, ASAP 2020) was used for the pore distribution and surface area of the sample. The BET surface area measurement method is used to measure the specific surface area of a material with small particles, such as clay particles using physical adsorption, desorption, and chemical adsorption and desorption, regardless of the material of the sample. The surface area can be obtained by adsorbing nitrogen on the particle surface, measuring the amount of adsorbed nitrogen gas, and calculating it using the bet formula. Adsorption is a phenomenon where gas molecules attach to the surface of a solid to become stable, and the surface of a solid becomes unstable when gas molecules are made to move in an irregular direction and speed [27]. Conversely, desorption means that the adsorbed molecules are separated (evaporated) from the surface. At this time, the volume of the gas can be calculated by measuring the pressure changed under certain conditions. The size of pores can be estimated by substituting the pressure change result from the specific surface area measurement into Equation (5) using the Kelvin equation below.

$$\ln \frac{p}{p_0} = -\frac{2\gamma V_a}{rRT} \cos \theta \quad (5)$$

Where: γ : surface tension r : radius of pore R :gas constant T : Kelvin temperature θ : contact angle

- (5) Single cell experimental apparatus:The charge/discharge test is performed by composing the system shown in Fig. 1. The electrolyte solution is composed of 1.6 M VOSO₄ and 4 M H₂SO₄, which is used by electrolytic reduction and a 25 cm² RFB battery was manufactured and used. The ion exchange membrane uses Nafion 212 from DuPont. In addition, in the tanks for storing and supplying the electrolytes of the cathode and anode, pumps are used to press the electrolyte into the cells of the cathode and anode respectively. The electrolyte solution enters the storage tank again after the cell is circulated. The flow rate is 15 mL/min, the current collector is a copper plate, and both ends are placed with graphite plates. For single cell analysis, use an automatic battery cycler (WBCS3000, WonA Tech) to charge to 1.75V and dscharge to 0.8V [28].

3. Results and discussion

3.1. Thermogravimetric analysis of carbon felt

Fig. 3 shows the TGA results of unthermaled carbon felt. Judging from the TGA chart from 25 °C to 800 °C the quality is somewhat degraded around 150–200 °C, this may be because the impurities and moisture contained in the carbon felt fall off or the evaporation of a fiber binder or hydrophobizing agent. Obvious weight loss occurs near 600 °C, which may be a rapid oxidation reaction of carbon. Thermal treatment above 600 °C shows that 600 °C is the temperature at which carbon felt officially begins to lose weight.

In order to improve the output power and energy efficiency of the redox flow battery, the reaction area (specific surface area) of the carbon felt used in the positive and negative electrodes should be increased, and the hydrophilicity should be improved to make the electrolyte flow well. For this, the oxidation method of thermaling in the air is used. In order to confirm the actual weight loss of the carbon felt after thermal treatment in the air, the weight loss rate of the thermal treatment of the carbon felt was calculated. The carbon felt was thermalmaled at temperatures of 300, 400, 500, 600, and 700 °C for 1, 2, and 3 h, and the weights before and after the thermal treatment were compared. The results are shown in Table-1.

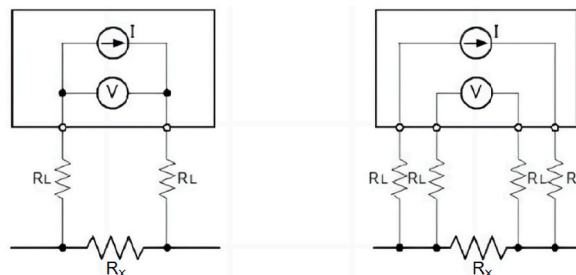


Fig. 2. Schematic diagram of the 4-terminal method and the 2-terminal method.

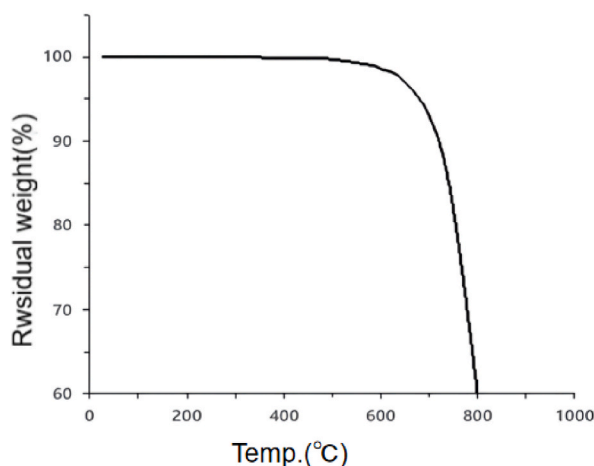


Fig. 3. TGA curve of untreated carbon felt (thermaling rate 5 °C/m.

Table 1

Weight loss of carbon felt by the thermal treatment at various temperature.

Temperature(°C)	thermaling time(h)	Weight loss(%)
300	1	0
	2	0
	3	0
400	1	0.05
	2	0.12
	3	0.24
500	1	0.26
	2	0.37
	3	0.55
600	1	2.85
	2	4.96
	3	8.21
700	1	11.5
	2	13.6
	3	17.3

3.2. The effect of thermal treatment on the structure of carbon felt

The results showed that Carbon felt thermal-treated at 300 °C shows negligible weight loss. At 400 °C, the weight loss for 1 h of thermaling time is very small, weight loss increases slightly with longer thermaling durations. Significant weight loss begins at 500 °C, with more substantial losses observed at 600 °C and 700 °C, indicating rapid oxidation at these higher temperatures. At 700 °C, the weight will be reduced by more than 10 % regardless of the time, so it cannot be used as an electrode. The results of the thermal treatment show that the weight of the carbon felt decreases sharply due to the rapid oxidation of carbon when the temperature is above 600 °C, so it can be inferred that the mechanical strength of the carbon felt will be weakened.

In order to study the effect of thermal treatment time on carbon felt based on the TGA results, the carbon felt was thermal treated at 300 °C, 400 °C, 500 °C, 600 °C and 700 °C for 2 h. After that, observe the surface by SEM. As shown in Fig. 4(a), the surface of the carbon felt thermal treated at 300 °C for 2 h showed a very smooth surface. As shown in Fig. 4(b), the surface of the carbon felt thermal-treated at 400 °C for 2 h also showed a smooth and clean appearance. As shown in Fig. 4(c), compared with other images, very small pores and a slightly rough surface can be seen in the carbon felt thermal-treated at 500 °C for 2 h. The SEM photos of Fig. 4(d) and (e) show that after thermal treatment at 600 °C and 700 °C for 2 h, the thickness of the carbon felt is greatly reduced due to rapid oxidation, and the surface will be severely deformed and damaged, showing that the mechanical strength is difficult to maintain. On this basis, the thermal treatment temperature range of carbon felt was reduced to 300–500 °C, and the surface area was measured by BET and compared.

Table 2 shows the BET measurement results of unthermaled carbon felt and thermal treatment at 300 °C, 400 °C, and 500 °C for 2 h. The carbon felt without thermal treatment is 0.59 m²/g, the carbon felt thermal-treated at 300 °C is 0.71 m²/g, thermal-treated at 400 °C is 1.92 m²/g, and thermal-treated at 500 °C is 4.38 m²/g. As the thermal treatment temperature increases, the specific surface area of the carbon felt increases significantly. It can be seen from the SEM photo in Fig. 4 that small pores are formed on the surface of the carbon felt, resulting in an increase in surface area.

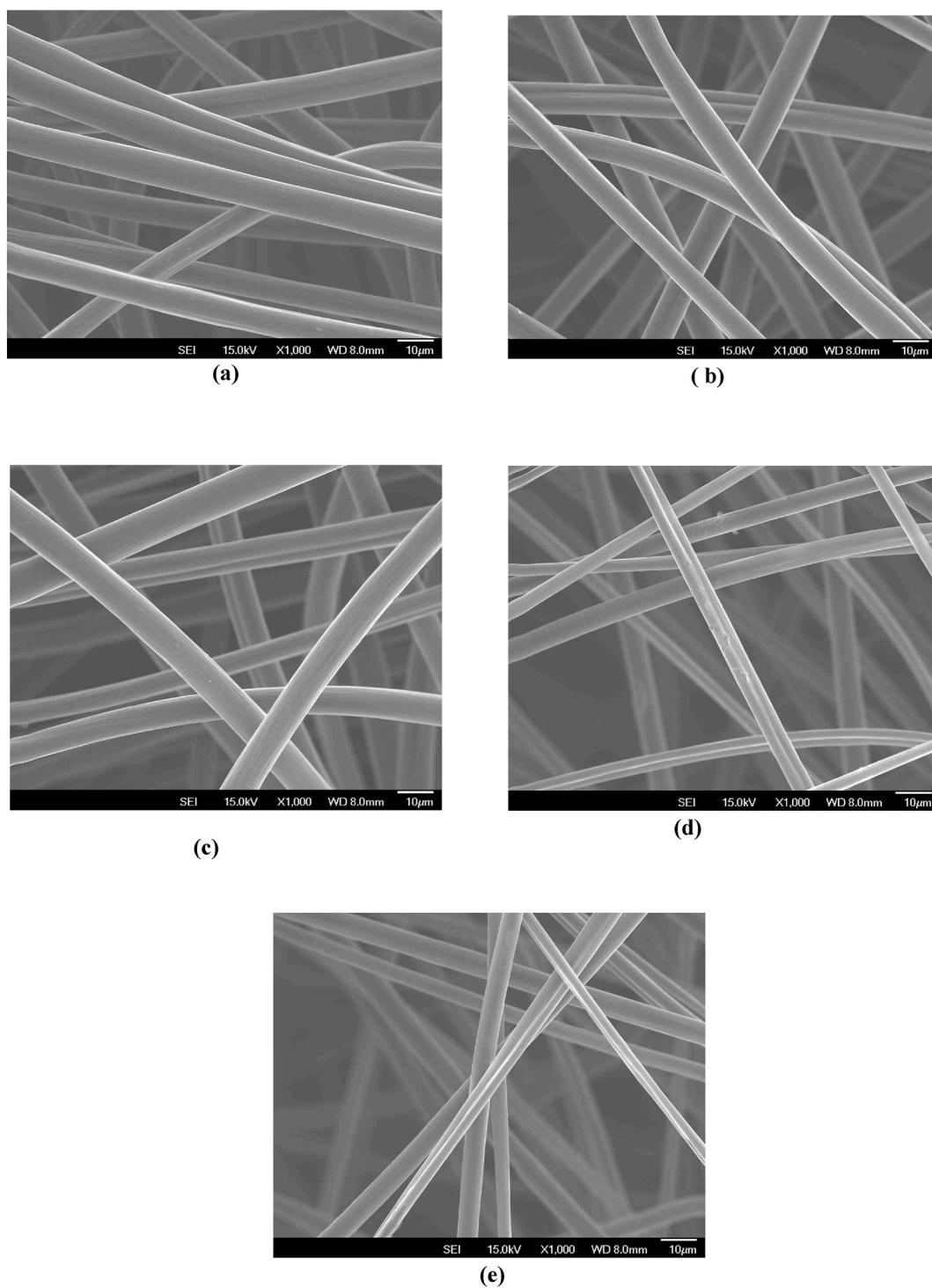


Fig. 4. SEM images of thermal treated carbon felt.(a)300 °C (b) 400 °C (c) 500 °C (d) 600 °C (e) 700 °C.

3.3. The effect of thermal treatment and pressure on the conductivity of carbon felt

One of the necessary conditions for carbon felt used in RFB is conductivity. Table 3 shows the electrical conductivity of the thermal-treated carbon felt. The carbon felt without thermal treatment is 8.32S/cm. As the temperature rises to 300 °C, 400 °C, the conductivity increases slightly, reaching to 9.15 S/cm, 9.23 S/cm, but thermal-treated at 500 °C the conductivity of the carbon felt reduced to 9.17

Table 2
BET surface area of carbon felt according to thermal temperature.

thermal temp.(°C)	BET surface area(m ² /g)
–	0.59
300	0.71
400	1.92
500	4.38

Table 3
Electrical conductivity of carbon felt according to the thermal treatment at various temperature.

thermal temp.(°C)	Electrical conductivity(S/cm)
–	8.32
300	9.15
400	9.23
500	9.17

S/cm, But its degree is minimal, within the margin of error. The results show that there is no significant relationship between thermal treatment temperature and conductivity.

In this experiment, when testing a single battery, pressure is applied up and down the device. In order to find the appropriate pressure, the carbon felt is compressed and the conductivity is measured. The compressibility of the carbon felt thermal-treated at 500 °C is 0–60 %. In order to measure the electrical conductivity, the samples shown in Table 4 are prepared, and the measurement results are shown in Fig. 5. It was found that the conductivity increased when the compression ratio reached 38 %, and the compression ratio higher than 38 % had no effect on the increase in conductivity. In addition, according to the report of Ghimire et al. , the pressure applied to the battery in the single-cell test is set to 25 kPa (compression rate 28 %). The report stated that the battery resistance increases with the increase in the compressibility of carbon felt [29].

3.4. Single test of thermal-treated carbon felt

Next, a single cell was manufactured using carbon felt thermal-treated at 300 °C, 400 °C, and 500 °C, and then a total of 20 charge/discharge cycles were performed. Among them, the last charge and discharge curve is shown in Fig. 6. Since the current in the charging test is fixed, the voltage at the start of charging is a factor that confirms the instantaneous resistance of charging, and the starting point of discharge is the voltage consumed as the transition to discharge occurs. That is, at the time of 0 s, where charging starts, the lower the voltage, the less the amount of loss. After the vertical drop at the start of discharge, the greater the voltage of the conversion part, the fewer the amount of loss when the charge is converted to discharge. It can be seen from the curve in this figure that the charging and discharging time of the carbon felt thermal-treated at 300 °C is the shortest. The carbon felt thermal-treated at 400 °C has the largest initial resistance, but the charging and discharging time is longer than that of the carbon felt thermal-treated at 300 °C. The carbon felt electrode thermal-treated at 500 °C showed the lowest charging start time (Onset potential) and the highest discharging start time (IRdrop). This means that since the resistance during charging and discharging is the lowest, the energy loss is the smallest, and it can be confirmed that the charging and discharging takes for the longest time, so the loss is the smallest in 20 cycles.

3.4.1. E.The effect of different catalysts and their addition methods on the characteristics of carbon felt

When the catalyst was applied to the carbon felt of the RFB electrode, experiments were carried out to study the change of the physical properties of the carbon felt and its influence on the electrode performance. Pt and Pd were selected as catalysts, and 20 wt% Pt/C and 20 wt% Pd/C were used as a raw material [30]. Two methods are used to incorporate the catalyst into the carbon felt. The carbon felt is first thermal-treated at 500 °C for 2 h. The first method is to use PTFE solution, Soak the carbon felt in a solution of 20 wt % Pt/C, Pd/C powder and PTFE, isopropanol, and water respectively [31]. Dry slowly at 40 °C (sample name: CF-PtTF, CF-PdTF).The second method is to use no PTFE solution, Soak the carbon felt in a solution of 20 wt% Pt/C,Pd/C powder and isopropanol and water

Table 4
Compression experiment of carbon felt.

Displacement (mm)	Sample thickness (mm)	Percentage compression(%)	Compressive pressure(kPa)
0	4.3	0	0
0.4	3.9	9.15	10.5
0.8	3.5	18.2	13.6
1.2	3.1	28	25.1
1.6	2.6	38	32.9
2.0	2.2	48	88.4
2.6	1.6	62	267.6

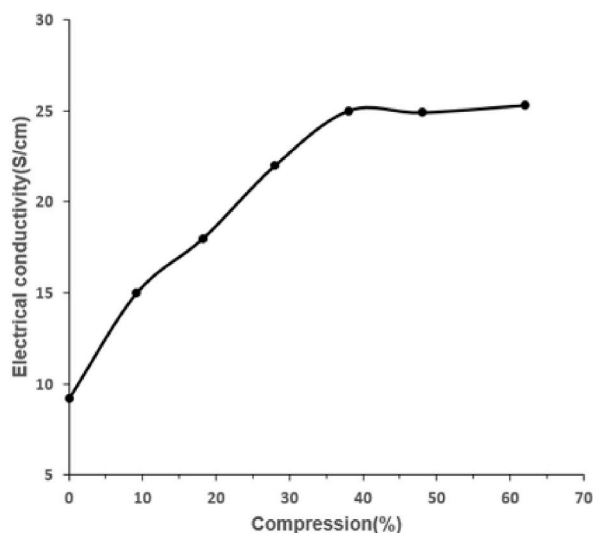


Fig. 5. Electrical conductivity of carbon felt thermaled at 500 °C, 2h

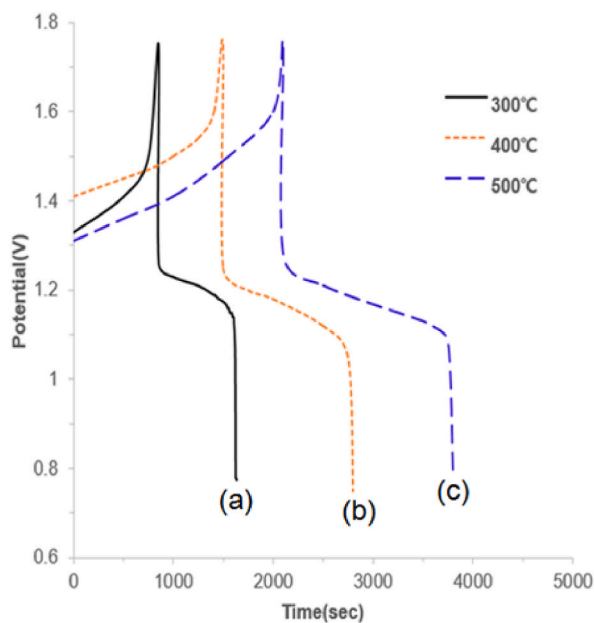


Fig. 6. Charge-discharge potential of single cell with thermaleled carbon felt electrode according to time(a)300 °C,(b)400 °C,(c)500 °C.

respectively, Dry slowly at 40 °C (sample name: CF-Pt, CF-Pd).Both methods make the final amount of Pt and Pd reach 5 wt% (vs. carbon felt). In each process, an ultrasonic homogenizer is used to ensure uniform dispersion. Table 5 shows the composition of carbon felt samples including Pt and Pd.

Fig. 7 shows the SEM images and EDS analysis of CF-PtTF and CF-PdTF, They contain catalysts using PTFE, It can be seen from the SEM photo that the PTFE contained and the carbon of the catalyst aggregate together. It is expected that the PTFE contained around the

Table 5
Sample preparation of carbon felt with catalyst.

Sample name	PTFE	Pt/C	Pd/C
CF-PtTF	○	20 wt%	×
CF-PdTF	○	×	20 wt%
CF-Pt	×	20 wt%	×
CF-Pd	×	×	20 wt%

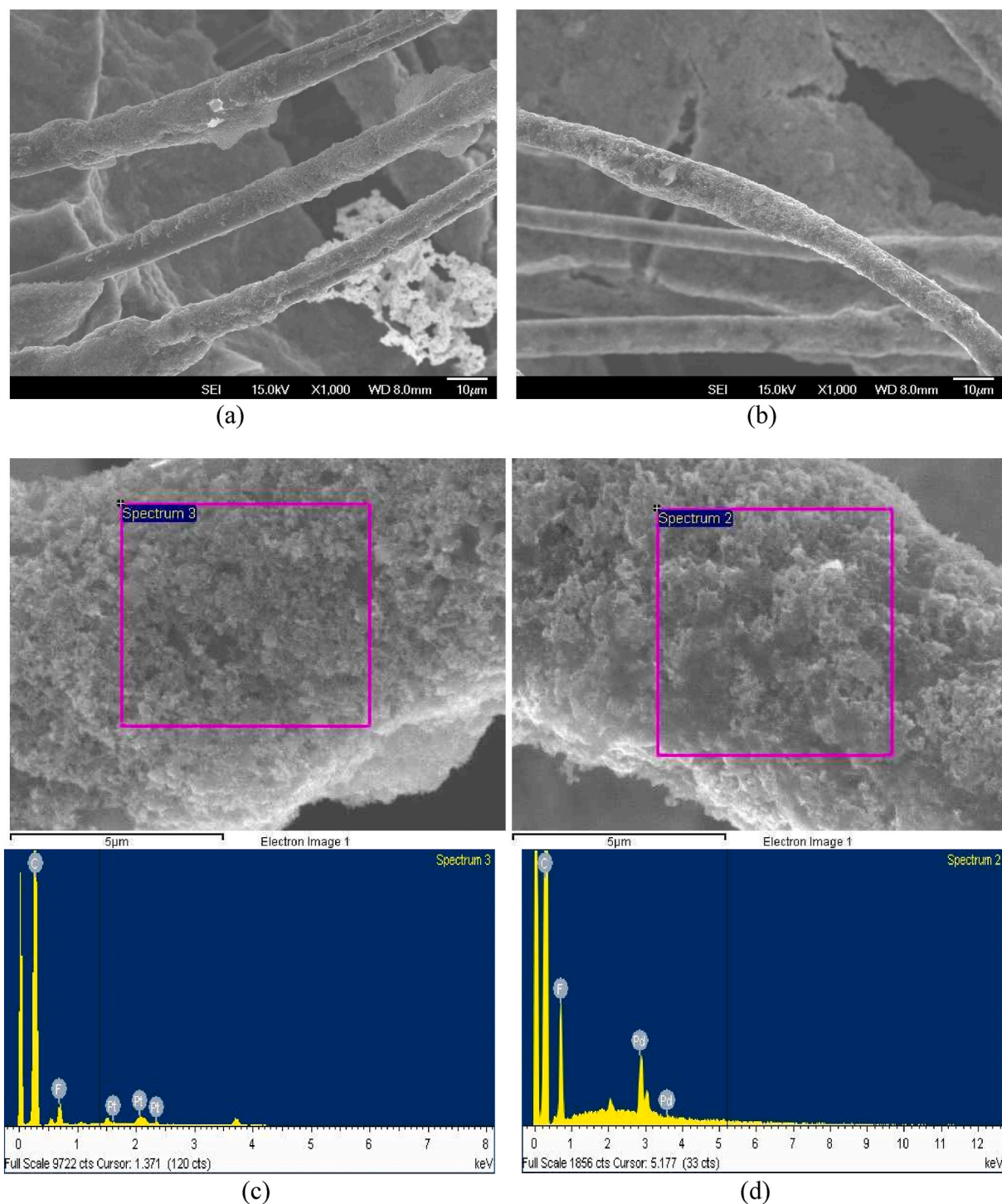


Fig. 7. SEM images and EDS analysis of carbon felt with catalyst.(a) CF-PtTF (b) CF-PdTF (c) CF-PtTF (d) CF-PdTF.

carbon felt and the carbon in the catalyst will condense together too much, which will hinder the electrode reaction. Fig. 8 shows the SEM images and EDS analysis of CF-Pt and CF-Pd, When it contains catalyst without using PTFE, The SEM picture shows that the catalyst-supported carbon is uniformly dispersed and adhered. From the SEM photos of Figs. 7 and 8, it is expected that when the catalyst is contained in the carbon felt, not using PTFE as a binder will not interfere with the electrode reaction.

Fig. 9 shows the electrical conductivity measurement results of CF-PtTF, CF-PdTF, CF-Pt, and CF-Pd to study the influence of the introduction of noble metal catalysts on the conductivity of carbon felt. Using a mixed solution of PTFE and catalyst carbon, the

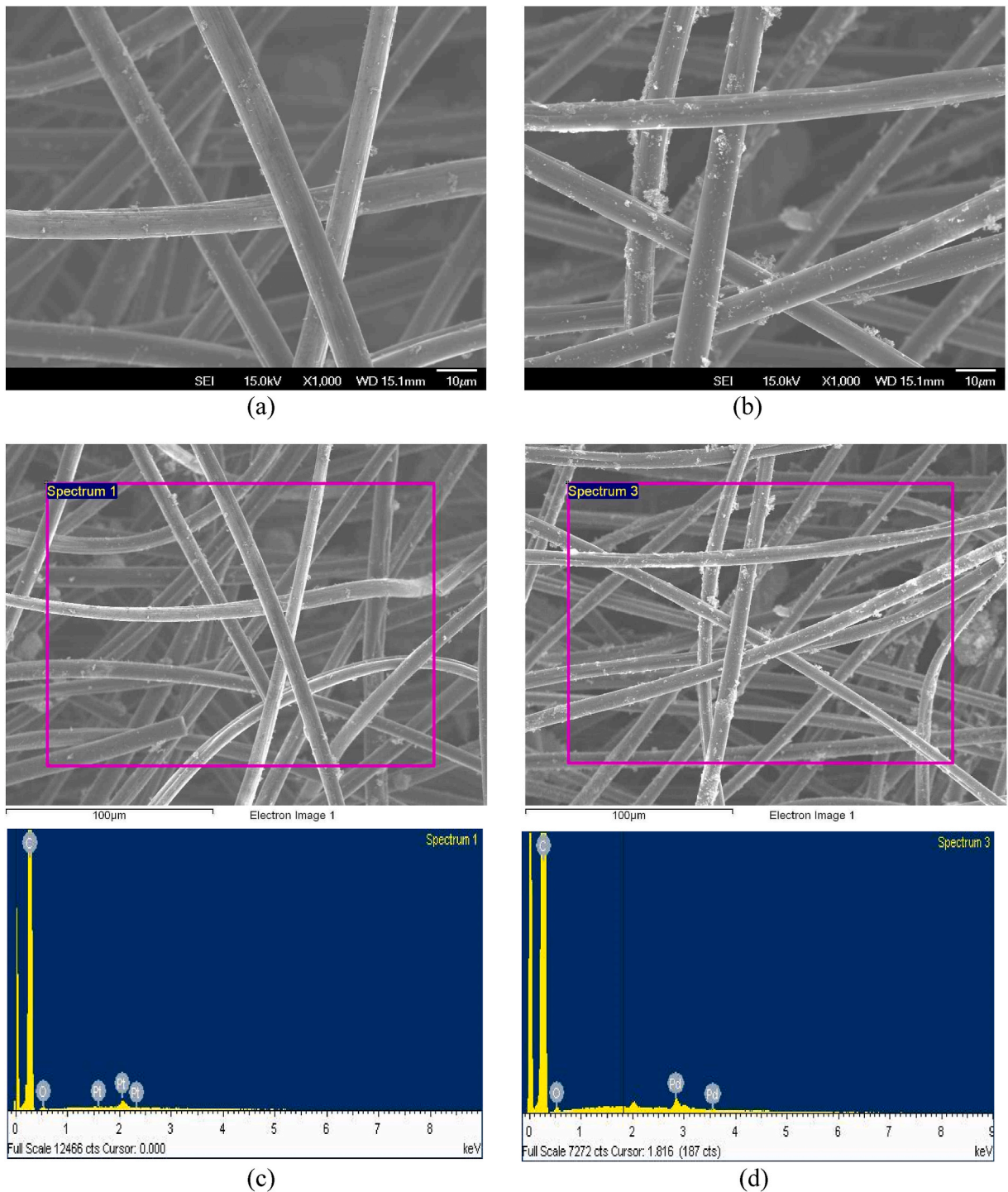


Fig. 8. SEM images and EDS analysis of carbon felt with catalyst.(a) CF-Pt (b) CF-Pd (c) CF-Pt (d) CF-Pd

conductivity of CF-PTFE and CF-PDTF is lower than that of carbon felt thermal-treated at 500 °C, this may be because PTFE hinders the conductivity of the carbon felt [32]. On the contrary, without using PTFE, the conductivity of CF-Pt and CF-Pd with catalyst is slightly higher than that of carbon felt thermal-treated at 500 °C. But from the structural point of view, adding Pt/C or Pd/C to carbon felt will not have much effect on its conductivity, it is because the physical structure of the carbon felt itself, such as its porosity and arrangement of carbon fibers, is the primary factor determining its conductivity. The addition of Pt/C or Pd/C, despite being conductive materials themselves, does not significantly alter the structure of the carbon felt in a way that would noticeably enhance or diminish its

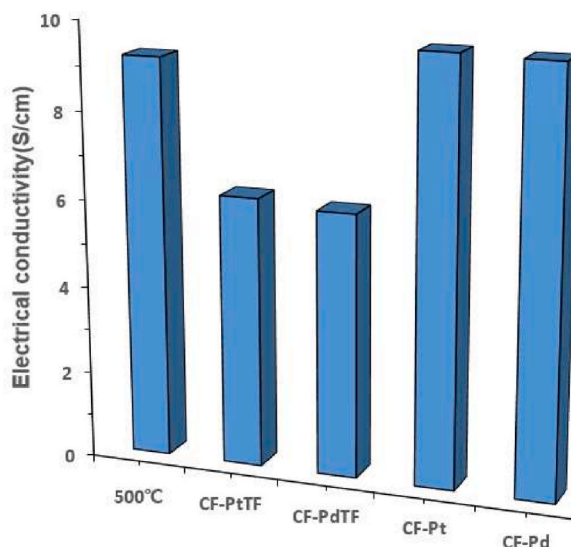


Fig. 9. Electrical conductivity of various carbon felt.

conductivity. Therefore, any changes in conductivity resulting from the addition of Pt/C or Pd/C would likely be minimal or negligible. Therefore the addition of Pt/C or Pd/C will not have much effect on the conductivity.

Table 6 shows the measurement results of the BET surface area of carbon felt and CF-PtTF, CF-PdTF, CF-Pt, CF-Pd thermal-treated at 500 °C. In the case of CF-PtTF and CF-PdTF containing catalysts using PTFE, the surface area of the carbon felt thermal-treated at 500 °C is reduced, As shown in the SEM photo, this is because the addition of PTFE caused the excessively aggregated paste to block the pores of the carbon felt. Without using PTFE, the CF-Pt and CF-Pd containing the catalyst have an increased surface area than the carbon felt thermal-treated at 500 °C, this is because the Pt/C and Pd/C attached to the surface of the carbon felt provide the reaction surface area respectively.

Fig. 10 shows the BET poresize distribution of untreated carbon felt (Notreated), CF-Pt and CF-Pd carbon felt. Compared with the untreated carbon felt, the pore area of the carbon felt containing Pt and Pd is significantly increased, Compared with Pd, Pt has a size distribution that is more conducive to active reactions.

Fig. 11 shows the charge/discharge diagram of a single cell using carbon felt thermal-treated at 500 °C, CF-Pt and CF-Pd as electrodes. Out of a total of 20 charge/discharge cycles, only the last cycle is shown. Compared with the carbon felt electrode thermal-treated at 500 °C, the initial resistance of CF-Pt and CF-Pd are both reduced, and the charging time and discharging time are also significantly increased. Carbon felt containing Pt has the lowest initial resistance, and shows slightly superior characteristics than carbon felt containing Pd in terms of initial resistance and charging/discharging time. Like the charge/discharge curves of carbon felts with different pretreatment temperatures, carbon felt electrodes containing Pt exhibited the lowest charging initiation voltage (initial potential) and the highest discharge initiation voltage (IR drop), this is the result of promoting the reaction by including Pt. Although it is not much different from the carbon felt using Pd, it can be seen that the platinum catalyst is more effective in terms of reactivity or resistance.

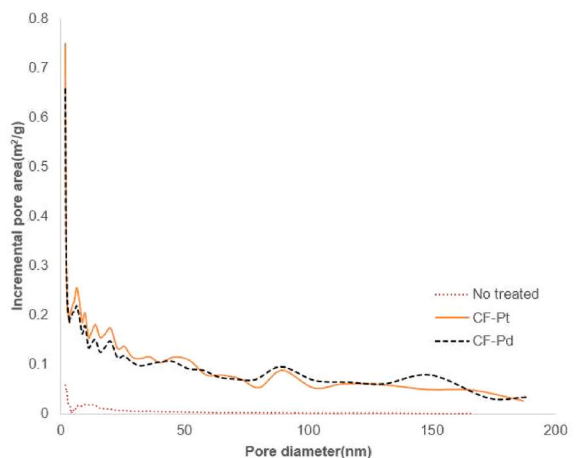
When comparing the size of the IR drop, the carbon felt electrode thermal treated at 500 °C showed 0.47V, CF-Pd showed 0.43V, and CF-Pt showed 0.41V. This is a result of accelerating the reaction by including catalysts. And the difference of performance with carbon felt using Pt and Pd catalyst is not very large, but carbon felt using Pt shows that it is more effective in reaction or resistance than carbon felt using Pd. The electrode containing Pt and Pd catalyst after thermal treated at 500 °C, 2h showed a smaller overvoltage and faster reaction rate compared to the electrode only thermal treated at 500 °C. When the overvoltage is low, the charge voltage is also low and the discharge voltage appears high, which determines the voltage efficiency.

4. Conclusion

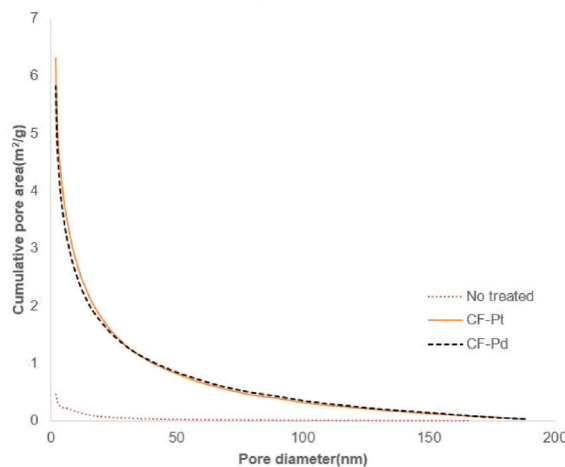
- (1) The carbon felt used as the electrode of the vanadium redox flow battery can increase the surface area by thermal treatment. Compared with the carbon felt without any treatment, the BET surface area of the carbon felt after 2 h of thermal treatment at 500 °C increased sharply from 0.59 m²/g To 4.38 m²/g. As the thermal treatment temperature of carbon felt increases, the BET surface area increases, but when the temperature exceeds 600 °C, due to rapid oxidation the thickness of the carbon felt is greatly reduced, which lead to the mechanical strength decrease.
- (2) By understanding the relationship between the thermal treatment temperature of the Carbon felt and the conductivity, it can be found that the conductivity of the Carbon felt without thermal treatment is 8.32S/cm, the thermal treatment at 300 °C is 9.15S/cm, the thermal treatment at 400 °C is 9.23S/cm, and the thermal treatment at 500 °C is 9.17S/cm, which has no significant relationship with temperature.

Table 6
BET surface area of various carbon felt.

Carbon felt	BET surface area(m ² /g)
no treated	0.59
500 °C thermal treated	4.38
CF-PtTF	2.15
CF-PdTF	1.96
CF-Pt	6.84
CF-Pd	6.53



(a)



(b)

Fig. 10. BET pore size distribution of carbon felts according to pore diameter (a) Incremental pore area (b) Cumulative pore area.

- (3) As a result of a single cell test with thermal-treated carbon felt as an electrode, when a carbon felt thermal-treated at 500 °C for 2 h is used as an electrode, the charge and discharge time is the longest and the resistance is the smallest. This may be because as the electrode surface area increases, the resistance decreases, and the reaction area increases.
- (4) 5 wt% of precious metals Pt and Pd are introduced into Carbon felt to improve electrode performance. When carbon containing precious metals is mixed with Carbon felt, without mixing the binder PTFE obtained a uniform and clean shape. In addition, the side where the binder PTFE is not mixed has excellent conductivity and BET surface area, and the cell performance is also excellent.
- (5) The addition of precious metals to Carbon can effectively improve the surface area and cell performance. Compared with Pd, the electrode resistance on the Pt side is lower, the charging and discharging time is longer, and the improvement effect on cell performance is greater. The electrode containing Pt and Pd catalyst after thermal treated at 500 °C, 2h showed a smaller overvoltage and faster reaction rate compared to the electrode only thermal treated at 500 °C.

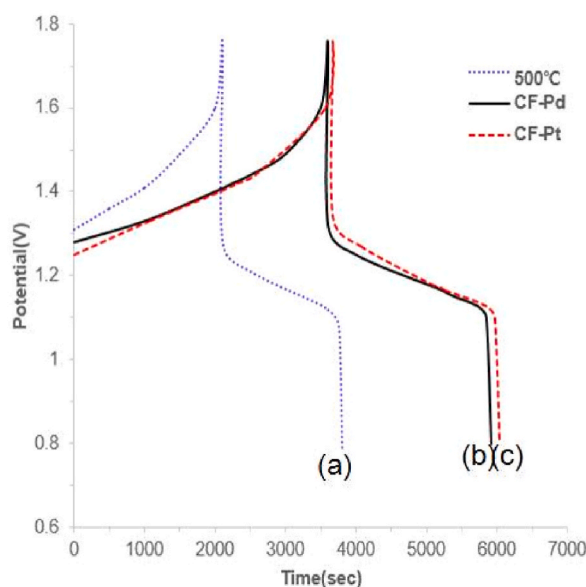


Fig. 11. Charge-discharge potential of single cell with various electrode according to time(a)500 °C,(b)CF-Pd,(c)CF-Pt

Data availability statement

The data included in article/supp. material/referenced in article used to support the findings of this study are available from the corresponding author upon request.

CRediT authorship contribution statement

Guanxia Dai: Writing – review & editing, Writing – original draft. **Yanhong Huang:** Funding acquisition, Data curation. **Feihong Chu:** Software, Investigation, Funding acquisition. **Chencong Jin:** Resources, Project administration. **Hui Liu:** Resources, Project administration, Funding acquisition.

Declaration of competing interest

We declare that we have no financial and personal relationships with other people or organizations that can inappropriately influence our work, there is no professional or other personal interest of any nature or kind in any product, service and/or company that could be construed as influencing the position presented in, or the review of, the manuscript entitled.

Acknowledgments

This work was funded by the Xingtai City Innovation Capacity Enhancement Plan Project (2023ZZ092 and 2023ZZ091), Hebei Natural Science Foundation (A2023108002), Xingtai City Key R&D Plan Project (2023ZC012), Hebei Province Higher Education Science and Technology Research Project (ZC2024149). We also acknowledge for the financial support from Xingtai Key Laboratory of New Energy Optoelectronic Devices and Energy Storage Technology.

References

- [1] D.M. Hall, R. Bachman, L.R. Radovic, Carbon materials in redox flow batteries: challenges and Opportunities, *Carbon* 201 (2023) 1241, 1241.
- [2] Z.B. Huang, A.L. Mu, Research and analysis of performance improvement of vanadium redox flow battery in microgrid: a technology review, *Int. J. Energy Res.* 45 (2021) 14170–14193, <https://doi.org/10.1002/er.6716>.
- [3] W. Wang, Q.T. Luo, B. Li, X.L. Wei, L.Y. Li, Z.G. Yang, Recent progress in redox flow battery research and Development, *Adv. Funct. Mater.* 23 (2013) 970–986, <https://doi.org/10.1002/adfm.201200694>.
- [4] I. Aramendia, U. Fernandez-Gamiz, A. Martinez-San-Vicente, E. Zulueta, J.M. Lopez-Guede, Vanadium redox flow batteries: a review oriented to fluid-dynamic optimization, *Energies* 14 (2021) 176, <https://doi.org/10.3390/en14010176>.
- [5] M.S. Yesilyurt, H.A. Yavasoglu, An all-vanadium redox flow battery: a comprehensive equivalent circuit model, *Energies* 16 (2023) 2040, <https://doi.org/10.3390/en16042040>.
- [6] A. Trovò, V. Di Noto, J.E. Mengou, C. Gamabaro, M. Guarnieri, Fast response of kW-class vanadium redox flow batteries, *IEEE Trans. Sustain. Energy* 12 (2021) 2413–2422, <https://doi.org/10.1109/Tste.2021.3096573>.
- [7] H. Sharma, M. Kumar, Energy efficient flow path for improving electrolyte distribution in a vanadium redox flow battery, *Int. J. Energy Res.* 46 (2022) 8424–8432, <https://doi.org/10.1002/er.7603>.

- [8] A. Bourke, D. Obozceanu, N. Quill, C. Lenihan, M.A. Safi, M.A. Miller, R.F. Savinell, J.S. Wainright, V. SasikumarSP, M. Rybalchenko, P. Amini, N. Dalton, R. P. Lynch, D.N. Buckley, Electrode kinetics and electrolyte stability in vanadium flow batteries, *J. Electrochem. Soc.* 170 (2023) 030504, <https://doi.org/10.1149/1945-7111/abc999>.
- [9] A.G. Olabi, M.A. Allam, M.A. Abdelkareem, T.D. Deepa, A.H. Alami, Q. Abbas, A. Alkhalidi, E.T. Sayed, Redox flow batteries: recent development in main components, emerging technologies, diagnostic techniques, large-scale applications, and challenges and barriers, *Batteries-Basel* 9 (2023) 409, <https://doi.org/10.3390/batteries9080409>.
- [10] P.C. Ghimire, A. Bhattarai, T.M. Lim, N. Wai, M. Skyllas-Kazacos, Q.Y. Yan, In-situ tools used in vanadium redox flow battery research-review, *Batteries-Basel* 7 (2021) 53, <https://doi.org/10.3390/batteries7030053>.
- [11] P. Arévalo-Cid, P. Dias, A. Mendes, J. Azevedo, Redox flow batteries: a new frontier on energy storage, *Sustain. Energy Fuels* 5 (2021) 5366–5419, <https://doi.org/10.1039/d1se00839k>.
- [12] W.X. Tian, H. Du, J.Z. Wang, J.J. Weigand, J. Qi, S.N. Wang, L.J. Li, A review of electrolyte additives in vanadium redox flow batteries, *Materials* 16 (2023) 4582, <https://doi.org/10.3390/ma16134582>.
- [13] A.W. Bayeh, D.M. Kabtamu, Y.C. Chang, T.H. Wondimu, H.C. Huang, C.H. Wang, Carbon and metal-based catalysts for vanadium redox flow batteries: a perspective and review of recent progress, *Sustain. Energy Fuels* 5 (2021) 1668–1707, <https://doi.org/10.1039/d0se01723j>.
- [14] Q.C. Jiang, Y.J. Ren, Y.J. Yang, L. Wang, L. Dai, Z.X. He, Recent advances in carbon-based electrocatalysts for vanadium redox flow battery: mechanisms, properties, and perspectives, *Compos. B Eng.* 242 (2022) 110094, <https://doi.org/10.1016/j.compositesb.2022.110094>.
- [15] K.E. Rodby, T.J. Carney, Y.A. Gandomi, J.L. Barton, R.M. Darling, F.R. Brushett, Assessing the levelized cost of vanadium redox flow batteries with capacity fade and rebalancing, *J. Power Sources* 460 (2020) 227958, <https://doi.org/10.1016/j.jpowsour.2020.227958>.
- [16] P. Loktionov, D. Konev, R. Pichugov, M. Petrov, A. Antipov, Calibration-free coulometric sensors for operando electrolytes imbalance monitoring of vanadium redox flow battery, *J. Power Sources* 553 (2023) 232242, <https://doi.org/10.1016/j.jpowsour.2022.232242>.
- [17] C. Ding, Z.F. Shen, Y. Zhu, Y.H. Cheng, Insights into the modification of carbonous felt as an electrode for vanadium redox flow batteries, *Materials* 16 (2023) 3811, <https://doi.org/10.3390/ma16103811>.
- [18] K.J. Kim, M.S. Park, Y.J. Kim, J.H. Kim, S.X. Dou, M. Skyllas-Kazacos, A technology review of electrodes and reaction mechanisms in vanadium redox flow batteries, *J. Mater. Chem. A* 3 (2015) 16913–16933, <https://doi.org/10.1039/c5ta02613j>.
- [19] C.H. Lin, Y.D. Zhuang, D.G. Tsai, H.J. Wei, T.Y. Liu, Performance enhancement of vanadium redox flow battery by treated carbon felt electrodes of polyacrylonitrile using atmospheric pressure plasma, *Polymers* 12 (2020) 1372, <https://doi.org/10.3390/polym12061372>.
- [20] K.V. Greco, A. Forney-Cuenca, A. Mularczyk, J. Eller, F.R. Brushett, Elucidating the nuanced effects of thermal pretreatment on carbon paper electrodes for vanadium redox flow batteries, *ACS Appl. Mater. Interfaces* 10 (2018) 44430–44442, <https://doi.org/10.1021/acsami.8b15793>.
- [21] X.J. Feng, Z.X. Zhang, T.X. Zhang, J. Xue, C. Han, L. Dai, L. Wang, Z.X. He, Enhanced catalysis of P-doped SnO for the V2+/V3+ redox reaction in vanadium redox flow battery, *Front. Chem.* 9 (2021) 688634, <https://doi.org/10.3389/fchem.2021.688634>.
- [22] A.M. Pezeshki, J.T. Clement, G.M. Veith, T.A. Zawodzinski, M.M. Mench, High performance electrodes in vanadium redox flow batteries through oxygen-enriched thermal activation, *J. Power Sources* 294 (2015) 333–338, <https://doi.org/10.1016/j.jpowsour.2015.05.118>.
- [23] Y.J. Ren, Y.J. Yang, J. Li, W.J. Zhu, J.Y. Gao, Y.G. Liu, L. Dai, L. Wang, Z.X. He, Synergistic catalysis of carbon/bismuth composite for V/V reaction in vanadium redox flow battery, *Ionics* 28 (2022) 4261–4271, <https://doi.org/10.1007/s11581-022-04663-8>.
- [24] J. Kim, H. Park, Experimental analysis of discharge characteristics in vanadium redox flow battery, *Appl. Energy* 206 (2017) 451–457, <https://doi.org/10.1016/j.apenergy.2017.08.218>.
- [25] L. Eifert, Z. Jusys, R.J. Behm, R. Zeis, Side reactions and stability of pre-treated carbon felt electrodes for vanadium redox flow batteries: a DEMS study, *Carbon* 158 (2020) 580–587, <https://doi.org/10.1016/j.carbon.2019.11.029>.
- [26] L. Garcia-Alcalde, A. Concheso, V.G. Rocha, C. Blanco, R. Santamaria, Z. Gonzalez, Influence of the oxygen surface functionalities introduced by electrochemical treatment on the behavior of graphite felts as electrodes in VRFBs, *Batteries-Basel* 8 (2022) 281, <https://doi.org/10.3390/batteries8120281>.
- [27] M.H. Chakrabarti, S.A. Hajimolana, F.S. Mjalli, M. Saleem, I. Mustafa, Redox flow battery for energy storage, *Arabian J. Sci. Eng.* 38 (2013) 723–739, <https://doi.org/10.1007/s13369-012-0356-5>.
- [28] J.F. Kucharyson, L. Cheng, S.O. Tung, L.A. Curtiss, L.T. Thompson, Predicting the potentials, solubilities and stabilities of metal-acetylacetonates for non-aqueous redox flow batteries using density functional theory calculations, *J. Mater. Chem. A* 5 (2017) 13700–13709, <https://doi.org/10.1039/c7ta01285c>.
- [29] P.C. Ghimire, A. Bhattarai, R. Schweiss, G.G. Scherer, N. Wai, Q.Y. Yan, A comprehensive study of electrode compression effects in all vanadium redox flow batteries including locally resolved measurements, *Appl. Energy* 230 (2018) 974–982, <https://doi.org/10.1016/j.apenergy.2018.09.049>.
- [30] T.M. Tseng, R.H. Huang, C.Y. Huang, K.L. Hsueh, F.S. Shieu, A kinetic study of the platinum/carbon anode catalyst for vanadium redox flow battery, *J. Electrochem. Soc.* 160 (2013) A690–A696, <https://doi.org/10.1149/2.073304jes>.
- [31] Z.X. He, Y.R. Lv, T.A. Zhang, Y. Zhu, L. Dai, S. Yao, W.J. Zhu, L. Wang, Electrode materials for vanadium redox flow batteries: intrinsic treatment and introducing catalyst, *Chem. Eng. J.* 427 (2022) 131680, <https://doi.org/10.1016/j.cej.2021.131680>.
- [32] L. Eifert, R. Banerjee, Z. Jusys, R. Zeis, Characterization of carbon felt electrodes for vanadium redox flow batteries: impact of treatment methods, *J. Electrochem. Soc.* 165 (2018) A2577–A2586, <https://doi.org/10.1149/2.053181jes>.